General Disclaimer

One or more of the Following Statements may affect this Document

- This document has been reproduced from the best copy furnished by the organizational source. It is being released in the interest of making available as much information as possible.

- This document may contain data, which exceeds the sheet parameters. It was furnished in this condition by the organizational source and is the best copy available.

- This document may contain tone-on-tone or color graphs, charts and/or pictures, which have been reproduced in black and white.

- This document is paginated as submitted by the original source.

- Portions of this document are not fully legible due to the historical nature of some of the material. However, it is the best reproduction available from the original submission.

GEOMETRY OF THE GEOMAGNETIC TAIL

KENNETH W. BEHANNON

APRIL 1969

GODDARD SPACE FLIGHT CENTER ——
GREENBELT, MARYLAND

GSFC

GEOMETRY OF THE GEOMAGNETIC TAIL

Kenneth W. Behannon
Laboratory for Space Sciences
NASA-Goddard Space Flight Center
Greenbelt, Maryland

April 1969

Abstract

An analysis of magnetic field measurements in the geomagnetic tail from Explorers 33 and 35 during 1967-1968 has shown that there is a broad region of depressed field magnitude approximately 12 R_E thick and centered on the neutral sheet. The solar magnetospheric B_Z component is proportionately larger within that region than outside of it. B_Z is found to decrease with distance from the earth but to be positive on average within the depressed field region out to a distance of 70 R_E, indicating that while for short periods of time the neutral line may be closer to the earth than the orbital distance of the moon, on average it is beyond that distance. A negative B_Z component was found in 2/3 of the measurements outside the depressed field region. This analysis has shown that the magnetotail field diverges on the order of 5° from the tail axis. This result together with the B_Z observations supports a geometry in which for large $|Z_{sm}|$ the tail field is diverging in the Z_{sm} as well as the Y_{sm} direction, but is converging slightly toward the neutral sheet within the depressed field region. The observed divergence produces an increase in the radius of the tail of approximately 3.8 R_E between distances of 20 R_E and 70 R_E from the earth. The combination of expanding tail and reconnection at the neutral sheet can account for an inverse power law field magnitude gradient of the form $B \propto |X|^{-0.3}$. The Explorer 33 and 35 measurements also indicate that the geomagnetic tail has an average aberration of 2.9 ± 0.2^O.

Introduction

The initial mapping of the magnetic field in the geomagnetic tail out to a distance of 31 R_E by IMP 1 established the basic structure of the tail. In addition to the generally steady, well-collimated nature of the field in the tail, a radius of approximately 20 R_E was deduced and the existence of a relatively thin ($\leq 1\ R_E$) neutral sheet separating oppositely directed fields was established (Ness, 1965; Speiser and Ness, 1967). Explorer 14 measurements showed a broad region of low field magnitude surrounding the field reversal region at a distance of 10-12 R_E (Cahill, 1966). Observations of electrons and protons with E > 100 eV by the Vela satellites at geocentric distances between 15.5 and 20.5 R_E showed that the plasma sheet surrounding the neutral sheet is often 4-6 R_E thick near the midnight meridian, increasing to approximately twice that thickness near the dusk and dawn boundaries (Bame et al., 1967).

Observations in the distant geomagnetic tail by Explorer 33 during 1966 showed that the tail is well-defined to a distance of 80 R_E (Ness et al., 1967a) and Pioneer 7 showed that it may extend as far as $10^3\ R_E$ (Ness et al., 1967b). It was found that the field magnitude decreases with distance from the earth, with a gradient that can be described by an inverse power law (Behannon, 1968a; Mihalov et al., 1968). The initially observed gradient has shown no statistically significant secular change (Mihalov and Sonett, 1968).

It has been suggested that the tail gradient must be the result
of either reconnection of field lines across the neutral sheet or
an increase in the radius of the tail with distance, or a combination
of the two mechanisms (Behannon, 1968a; Mihalov et al., 1968). The
early Explorer 33 data further suggested that the tail may not be
circular in cross-section but rather is elliptical with the major
axis in the Z_{sm} direction (Behannon, 1968a). All of these basic
features of the tail field topology have been reviewed in detail by
Ness (1969) and by Behannon and Ness (1969).

Explorer 35, in orbit about the moon since July 1967, spends
approximately 3.5 days in the magnetic tail each month. An analysis
of Explorer 35 magnetic field data has shown that no variations
due to an intrinsic lunar field are detected in the data when the
spacecraft is in the geomagnetic tail (Behannon, 1968b). The
Explorer 35 data have provided the most extensive mapping to date
of both the tail field in the plasma sheet region and the location
of the tail boundary at a constant distance down the tail from the
earth. This investigation combines the Explorer 35 tail field
measurements with those of Explorer 33 for the period July 1967-August
1968. Evidence is presented for the existence of:

     1. A broad region of depressed field magnitude and
        increased B_Z component surrounding the neutral sheet;

2. A slight divergence of tail field lines with distance from the earth; and

3. An aberration of the tail axis.

The location of the neutral sheet relative to the solar magnetospheric XY plane is discussed and the contributions of the expansion of the tail and the reconnection at the neutral sh et to the observed gradient are considered.

Data Distribution

The statistical portion of this investigation used a total of 2085 hours of combined Explorer 33 and Explorer 35 magnetic field data in the form of hourly average magnitudes and direction angles. The angles were computed from the hourly average solar magnetospheric cartesian components of the field. Only those averages for which $-70 \leq X_{sm} \leq -20$ R_E were used. For location of magnetopause and neutral sheet traversals 81.81 sec averages of the total vector measurements were utilized.

One third of the hourly averages used for the statistics corresponded to values of Kp > 2. Of those for which Kp $\leq$ 2, 72% were for $X_{sm} < -50$ R_E due to the contribution of Explorer 35 at the distance of the moon. A median tail field magnitude of 8.9γ was computed for all data for which Kp $\leq$ 2; however, this average is not very meaningful as an average for the entire tail because of the distance bias in the data. A median magnitude of 11.8γ was obtained from the data for which Kp > 2.

More meaningful are magnitude distributions for a limited range of X_{sm}, especially in the distant tail where the magnitude gradient is small. Such distributions are shown in Figures 1 and 2 for $-65 \leq X_{sm} \leq -55$ R_E. Figure 1 shows a partitioning of the data by Kp $\leq$ 2, > 2, and Figure 2 partitions the data by Z_{sm} range for Kp $\leq$ 2. A difference of 2.3γ in median magnitude was found for

separation by Kp. In Figure 2 it is seen that a broad distribution is found for an inner region 12 R_E thick in the Z_{sm} direction and centered at Z_{sm} = +2 R_E, whereas a more peaked distribution is found outside that region. The inner region had a median magnitude which was 1.7γ lower than that for the outer region. For the same geometry the difference is 2.2γ for the full range of -70 ≤ X_{sm} ≤ -20 R_E. In the still smaller core region 0 ≤ Z_{sm} ≤ 5 R_E, within which 2/3 of the neutral sheet observations occurred, a median magnitude of 7.0γ was found for 357 hours of data with -70 ≤ X_{sm} ≤ -20 R_E.

Depressed Field Region

The region $0 \leq Z_{sm} \leq 5$ R$_E$ is seen as the region of lowest average field magnitude in Figure 3. This figure demonstrates the existence of a broad region of depressed magnetic field magnitude in the geomagnetic tail near the solar magnetospheric equatorial plane. The data in Figure 3 consist of 1346 hourly averages for which $-70 \leq X_{sm} \leq -20$ R$_E$ and Kp ≤ 2. Plotted in the top portion of the figure are averages of the hourly magnitude values for each 2 R$_E$ interval of Z_{sm}. The RMS magnitude deviations corresponding to each of the 2 R$_E$ magnitude averages are shown in the lower part of the figure.

Vertical lines at $Z_{sm} = \pm 8$ R$_E$ suggest that the depressed region is asymmetric with respect to $Z_{sm} = 0$. Because Explorer 33 is in the tail only during the months May through October, more than 2/3 of the data used for Figure 3 were from measurements performed during those months. Indeed there is very little difference between Figure 3 and a comparable figure for the summer data alone. However, as will be shown, 11 out of 13 intervals of neutral sheet observations by Explorer 35 during the winter months November to January occurred at $Z_{sm} > 0$.

The RMS values in Figure 3 show some tendency to decrease for large values of $|Z_{sm}|$. However, the distribution is in general relatively flat, especially within the depressed field region, with

the highest values near the boundaries of that region. This suggests
that the low magnitude portion of Figure 3 is not produced solely
by a thin low field region constantly in motion throughout the
broader region but rather by a physically real, broad depressed
region which itself exhibits motion at its upper and lower
boundaries. The average depressed region is approximately 12 R_E
thick, which is consistent with the plasma sheet thickness near
the dawn and dusk boundaries of the tail (Bame et al., 1967).

Another feature of the depressed magnitude region is the
tendency for the B_Z component of the field to be larger within the
region than outside. This is illustrated in Figure 4 where the
elevation angle of the field θ_{sm} is shown as a function of the
Z_{sm} position of the measurement. The figure summarizes 1120 hours
of data. The $\pm 90^\circ$ range of θ_{sm} has been subdivided into 12 intervals
corresponding to equal area latitude regions of a spherical surface.
The number of cases of hourly values of θ_{sm} falling within each
angular interval as well as within 2 R_E intervals of Z_{sm} has been
tabulated, and the θ_{sm} and Z_{sm} marginal distributions are also given.

Figure 4 illustrates not only the thickness of the region in
which the B_Z component of the field is a significant fraction of the
total field but also the essentially positive character of the
B_Z component for $-70 \leq X_{sm} \leq -20$ R_E. Negative values of B_Z are found

to predominate only for $|Z_{sm}|$ large. This suggests that whereas the magnetic field lines tend to converge toward the neutral sheet in the plasma sheet region, at large values of $|Z_{sm}|$ the field diverges slightly. This is consistent with a slight divergence which is found to occur in the $\pm Y_{sm}$ directions. This will be discussed in a later section.

Seventy-five percent of the depressed field region data in Figure 4 correspond to a positive B_Z component. Since 72% of the data used in Figure 4 correspond to values of $X_{sm} < -50 R_E$, the predominance of positive B_Z on the average in the plasma sheet region as tabulated in the figure supports the conclusion that the neutral line is generally beyond the region of the data, i.e., beyond $X_{sm} = -70 R_E$.

Location of the Neutral Sheet

Speiser and Ness (1967) suggested that because the neutral sheet begins near the geomagnetic equatorial plane, one might expect to find that the change of tilt of the magnetic dipole between June and December would shift the neutral sheet from above to below the solar magnetospheric equatorial plane. The Explorer 35 neutral sheet traversal data were investigated for evidence of this seasonal shift of position. Unfortunately during the summer when the neutral sheet should be above the solar magnetospheric XY plane the moon is generally located below that plane, and the opposite is true for the winter months. However, traversals of the neutral sheet by Explorer 35 did occur, and for random motions of the sheet and equal numbers of hours of observations during the two seasons one would expect approximately symmetrical distributions of traversal locations.

Figure 4 shows the locations of points on the $Y_{sm} Z_{sm}$ plane where Explorer 35 observed at least one clear field reversal while passing through the tail during both northern hemisphere summer months (May-July 1967) and winter months (November 1967-January 1968). During those periods there were 192 hours of winter data and 201 hours of summer data. Thus there were approximately equal numbers of hours in each seasonal interval. Along the sides of the figure are plotted the distributions of the data as functions of Z_{sm} position for the summer (left) and winter (right) periods. As can

be seen, these distributions have similar profiles with peaks
at approximately $Z_{sm} = \pm 5 R_E$.

Even though a high degree of symmetry existed in the sampling,
out of 18 clear occurrences of single or multiple neutral sheet
traversals, only 5 such events were observed below the $Y_{sm}Z_{sm}$ plane.
This implies that at the lunar distance during these periods the
neutral sheet tended to have a Z_{sm} coordinate more positive than
negative on the average, even during the winter months.

Divergence and Aberration of Tail Field

Mihalov et al. (1968) have reported that in 1966 the geomagnetic tail field observed by Explorer 33 tended to have a component toward the dawn side of the tail, both above and below the field reversal region. This "skewing" of the tail field, which was found to be more pronounced near the field reversal region, was attributed to a twisting of field lines.

The results of this present analysis of data from Explorers 33 and 35 are consistent with the view that angular deviations of tail field lines from the sun-earth direction are produced both by a spreading of the tail field with distance from the earth and an aberration of the tail due to the earth's motion about the sun.

Shown in Figure 6 are 1262 hourly values of the field azimuthal angle φ_{sm} as a function of Y_{sm} across the tail. Data from both below the field reversal region and above it are folded together so that the angle between the field and the earth-sun line in the $X_{sm}Y_{sm}$ plane is plotted whereas the polarity of the field, either toward or away from the earth, is not considered. Thus hours for which φ_{sm} was 190° and 010° would have the same abscissa.

An appreciable number of cases are seen in which the field made a large angle with the $360^\circ/180^\circ$ direction. These points are from the plasma sheet region where the direction is found to fluctuate widely. Even with the greater scatter due to those

points being included, the general trend of the data is unmistakable.
When only data for which $|Z_{sm}|$ is large are used the trend of the
data is even more obvious.

A least squares fit to the plotted data is shown. It reveals
two significant features of the distribution. The negative-slope
tilt of the distribution can be interpreted as resulting from the
divergence of the field away from the tail axis with distance from
the earth. A line with positive slope would result from converging
field lines, whereas a configuration in which all the field lines
on one side of the neutral sheet are deviated to the west and those
on the other side to the east would result in two separate distributions,
both parallel to the $360^{o}/180^{o}$ line. The data were separated into
measurements below the field reversal and those above it, and the
result was the same in each case as that shown in Figure 6 for the
combined data. Thus the distance of field lines from the X_{sm} Z_{sm}
plane is increasing with distance from the earth on both sides of
that plane and both above and below the neutral sheet. The
divergence is found to be greater inside the plasma sheet region
than outside.

The second significant feature of the data is the tendency for
field lines with direction $360^{o}/180^{o}$ to be located at a negative
value of Y_{sm} (the point where the linear fit to the data crosses the

$360^{\circ}/180^{\circ}$ line). This reflects the aberration of the tail axis
west of the antisolar direction as viewed from the earth. An average
aberration of 2.7° is obtained from this analysis. The divergence,
together with the aberration, results in an average solar-magnetospheric
azimuthal angle for the field of $\varphi_{sm} = 187^{\circ}$ at $Y_{sm} = - 20 R_E$ and
170° at $+ 20 R_E$.

Another approach to obtaining a value for the average
aberration is through analysis of the tail boundary traversal data.
This also can yield information on the shape and size of the tail
cross-section. Figure ⸳ ⸳ summarizes such traversal data for
Explorers 33 and 35 during 1967-1968. The line segments plotted
represent periods during which a series of multiple crossings were
observed. They are projections of the trajectories on the $Y_{sm}Z_{sm}$
plane. The single point on the positive Y_{sm} side of the tail
represents a case of only one traversal being seen. The two points
on the negative Y_{sm} side are final traversals in series of multiple
traversals where the initial crossings were not clearly distinguishable
from neutral sheet effects.

A non-linear least squares fit of a circular cross-section to
the mean traversal points results in an aberration of 3.1° and a
radius of $23.8 R_E$ at the distance of the moon. An aberration of
2.7° was obtained by the other independent method. Strong et al.,

- 14 -

(1967) reported that from July 1964 to July 1965 the solar wind velocity had an average component from 1.4° east of the sun, corresponding to an azimuthal velocity of 10 km/sec. When this is added to a tail aberration angle of $2.9 \pm 0.2^\circ$ one obtains a value of 397 ± 18 km/sec for solar wind velocity.

According to Burlaga (private communication) Explorer 34 solar wind observations have not found the azimuthal component to be as large as that reported by Strong et al. from the Vela 2A and 2B observations. Brandt et al. (1969) state that an azimuthal velocity of 2.5 km/sec in the vicinity of the earth is consistent with quiet time comet data. Explorer 34 found the solar wind to have an average velocity of 440 km/sec for eight months of observations in 1967 (Burlaga, private communication). This value together with an average aberration of 2.9° suggests an average solar wind velocity from 1.0° east of the sun.

Although a circular cross-section was drawn to the boundary traversal data in Figure 7, as can be seen there were multiple traversals of the boundary by Explorer 33 at large negative values of Z_{sm}. As was noted in 1966 (Behannon, 1968a) the southern boundary of the tail is generally encountered at values of Z_{sm} near -30 R_E, suggesting an elliptical cross-section for the tail with greater breadth in the Z_{sm} than in the Y_{sm} direction by

approximately 3 to 2. This is consistent with a tail

consisting of two approximately circular bundles of flux from

the polar caps aligned adjacent to one another. It should be

noted, however, that one complete pass by Explorer 33 in 1968

just inside a radius of 30 R_E failed to contact the tail a single

time.

Contributions of Field Line Divergence and Reconnection to the Magnitude Gradient.

It has been shown that the geomagnetic tail field diverges slightly with distance from the earth. If this results in an increase in the radius of the tail with distance, then the divergence will contribute to the observed magnitude gradient, in addition to any contribution through loss of flux due to reconnection across the neutral sheet or at the boundary. The tail radius has been shown to be approximately 23.8 R_E near a distance of $X_{sm} = -60 R_E$. This is 3.8 R_E greater than the average radius of 20 R_E found near $X_{sm} = -20 R_E$. An increase of that magnitude would result from an angle of $5°$ between the tail boundary and the tail axis. This is not inconsistent with the results of the φ_{sm} analysis.

If one assumes that only the divergence of the tail is effective in producing a magnitude gradient, than the average magnitude B_2 at a given distance down the tail, where the radius is R_2, is obtained in terms of the magnitude B_1 at a point where the radius is R_1 $(R_2 > R_1)$ by using the invariance of the magnetic flux. This gives

$$\Phi_2 = \Phi_1$$
$$\text{or } B_2 A_2 = B_1 A_1$$

where A_1 and A_2 are the cross-sectional areas at distances of X_1 and X_2, respectively. Hence

$$B_2 = B_1 \frac{R_1^2}{R_2^2}$$

$$\text{or} \quad B_2 = B_1 \frac{R_1^2}{(R_1 + \Delta X \tan\alpha)^2}$$

where $\Delta X = X_2 - X_1$ and α is the angle between the tail boundary and the tail axis. Using this relationship and $\alpha = 5^{\circ}$ curve A in Figure 8 was computed. The solid curve in the figure is the inverse power law $B \propto |X|^{-0.3}$ found for the 1966 data (Behannon, 1968a). The value from the observed gradient at $X_{sm} = -20 R_E$ was used as the initial value for curve A. As can be seen, a 5° divergence of the tail does not by itself cause the magnitude to decrease with distance in a manner consistent with the observed gradient.

Curve B, which is a simple model of the reconnection gradient, is also seen to be unable alone to account for the observed gradient. Curve B was calculated using average solar magnetospheric B_Z components observed in the range $0 \leq Z_{sm} \leq 5 R_E$ for $Kp \leq 2$. Averages of the hourly B_Z values were computed for each 10 R_E interval of X_{sm} for $-70 \leq X_{sm} \leq -20 R_E$. These averages were:

for X distance = 20-30:	$B_Z = 3.52\gamma$
30-40:	1.87γ
40-50	1.01γ
50-60:	0.69γ
60-70:	0.55γ

A calculation of the gradient was made using conservation of flux:

$$\Phi_2 = \Phi_1 - \Phi_Z$$

where Φ_1 and Φ_2 are fluxes through semi-circular cross-sections of the tail at distances X_1 and X_2 ($X_2 > X_1$) and Φ_Z is the flux lost in reconnection at the neutral sheet between X_1 and X_2. Then for a tail of constant radius and hence constant cross-sectional area A,

$$B_2 = B_1 - B_Z \frac{A_{XY}}{A}$$

where A_{XY} is the area of the neutral sheet between X_1 and X_2 and B_Z is the average normal field component over that area. Using this highly simplified model and the observed average B_Z values, gradient B was calculated.

Since it is clear that both gradient-pro cing mechanisms are contributing to the tail gradient, the combined effect was computed using

$$B_2 = B_1 \frac{R_1^2}{(R_1 + \Delta X \tan \alpha)^2} - B_Z \frac{A_{XY}}{A(X)}$$

in which the cross-sectional area $A(X)$ is now increasing with distance down the tail in accordance with the 5° divergence of the

tail boundary, This calculation at 10 R_E intervals along the
tail produced curve A+B in Figure 8. As can be seen, even this
simple approach can produce a gradient that is consistent with the
inverse power law $B \propto |X|^{-0.3}$.

Summary

An analysis of measurements in the geomagnetic tail during 1967-1968 has shown that there is a broad region approximately 12 R_E thick centered on the neutral sheet in which the field magnitude is depressed and the B_Z component of the field is a larger fraction of the total field than outside the region. During the period of the data both the depressed magnitude region and the neutral sheet were on the average centered above the solar magnetospheric equatorial plane. For all data for which $-70 \le X_{sm} \le -20 \; R_E$ and $Kp \le 2$, the median magnitude inside such a broad region centered at $Z_{sm} = 4 \; R_E$ was found to be approximately 2γ less than the median magnitude outside the region. The depressed region agrees quite well with the region in which the plasma sheet was detected by Vela spacecraft near 17 R_E (Bame et al., 1967).

This analysis also has revealed a slight spreading of the tail field with distance down the tail. The existence of a field component normal to the tail magnetopause has not yet been established experimentally. If the tail field is generally tangent to the boundary then the analysis suggests that the radius of the tail increases with distance between $X_{sm} = -20 \; R_E$ and $X_{sm} = -70 \; R_E$. Boundary traversal observations at the distance of the moon indicate that the increase is not greater than 3.8 R_E. The data were

investigated for a systematic variation of the field divergence
with distance down the tail, but none could be detected.

The average solar magnetospheric B_Z component of the field
in the depressed field region was found to decrease with distance
from the earth. The average B_Z component was negative only 25%
of the time within that region while outside the region it was
negative 67% of the time. These data support the view that in the
Z_{sm} direction the field is converging and reconnecting within
the plasma sheet and diverging outside that region, with the neutral
line generally beyond the orbit of the moon. These results do not
support the suggestion by Dessler (1968) that the neutral line is
as near to the earth as 20 R_E.

The expansion of the tail with distance and the reconnection
at the neutral sheet both contribute to the field magnitude gradient
in the tail. Simple flux corsiderations lead to a gradient from the
two mechanisms that is in good agreement with a gradient proportional
to $|X|^{-0.3}$. Such a gradient was found to describe the 1966 Explorer
33 measurements (Behannon, 1968a). However, Mihalov and Sonett
(1968) reported gradients of $B \propto |X|^{-0.736}$ and $B \propto |X|^{-0.798}$,
respectively, from analyses of 1966 and 1967 tail data. These
differ from the results reported by Behannon predominantly in the
steepness of the gradient at the near-earth end of the tail. A

gradient was not computed for the data used in this current analysis because of the sparseness of the data near X_{sm} = -20 R_E, which is the most critical region in accurately establishing the correct exponent in the assumed power law variation.

If the gradient is much steeper than that shown in Figure 8 then it is obvious that the results used in this analysis would not suffice to describe the magnitude decrease. Either a larger B_Z component at a distance of 20-30 R_E or a considerably larger increase in the radius of the tail with distance, or again a combination of both effects, would be required to account for such a steep decrease, unless it is due to reconnection at the magnetopause.

This investigation has found an average aberration of the tail of $2.9^{\circ} \pm 0.2^{\circ}$ based on two independent methods of analysis. An average solar wind velocity of 440 km/sec is obtained from such an aberration if the solar wind has a component from 1.0° east of the sun.

The analysis of tail boundary traversal data supports previous evidence that the tail is not actually circular in cross-section but rather is elliptical with the semi-major axis oriented along the solar magnetospheric Z axis.

Acknowledgements

- 24 -

References

Bame, S. J., J. R. Asbridge, H. E. Felthauser, E. W. Hones and I. B. Strong, Characteristics of the Plasma Sheet in the Earth's Magnetic Tail, J. Geophys. Res., 72, 113, 1967.

Behannon, Kenneth W., Mapping of the Earth's Bow Shock and Magnetic Tail by Explorer 33, J. Geophys. Res., 73, 907, 1968a.

Behannon, Kenneth W., Intrinsic Magnetic Properties of the Lunar Body, J. Geophys. Res., 73, 7257, 1968b.

Behannon, Kenneth W., and Norman F. Ness, Satellite Studies of the Earth's Magnetic Tail, Physics of the Magnetosphere, Ed. by R. L. Carovillano, J. F. McClay and H. R. Radoski, D. Reidel Publishing Company, Dordrecht, Holland, 1969.

Brandt, John C., Charles Wolff, and Joseph P. Cassinelli, Interplanetary Gas XVI. A Calculation of the Angular Momentum of the Solar Wind, Ap. J., 155, June 1969.

Cahill, L. J., Inflation of the Magnetosphere Near 8 Earth Radii in the Dark Hemisphere, Space Research, Vol. VI, 662, 1966.

Dessler, A. J., Magnetic Merging in the Magnetospheric Tail, J. Geophys. Res., 73, 209, 1968.

Mihalov, J. D., D. S. Colburn, R. G. Currie, and C. P. Sonett, Configuration and Reconnection of the Geomagnetic Tail, J. Geophys. Res., 73, 943, 1968.

Mihalov, J. D. and C. P. Sonett, The Cislunar Geomagnetic Tail Gradient in 1967 (letter), J. Geophys. Res., 73, 6837, 1968.

Ness, Norman F., The Earth's Magnetic Tail, J. Geophys. Res., 70, 2989, 1965.

Ness, Norman F., The Geomagnetic Tail, Reviews of Geophysics, 7, February 1969.

Ness, N. F., K. W. Behannon, S. C. Cantarano, and C. S. Scearce, Observations of the Earth's Magnetic Tail and Neutral Sheet at 510,000 Kilometers by Explorer 33, J. Geophys. Res., 72, 927, 1967a.

Ness, Norman F., Clell S. Scearce and Sergio C. Cantarano, Probable Observations of the Geomagnetic Tail at 10^3 R_E by Pioneer 7, J. Geophys. Res., 72, 3769, 1967b.

Speiser, T. W. and N. F. Ness, The Neutral Sheet in the Geomagnetic Tail: Its Motion, Equivalent Currents, and Field Line Reconnection Through It, J. Geophys. Res., 72, 131, 1967.

Strong, I. B., J. R. Asbridge, S. J. Bame and A. Hundhausen, Satellite Observations of the General Characteristics and Filamentary Structure of the Solar Wind, The Zodiacal Light and the Interplanetary Medium, Ed. by J. L. Weinberg, Scientific and Technical Information Division, Office of Technology Utilization, National Aeronautics and Space Administration, Washington, D. C. 1967.

Figure Captions

Figure 1 Geomagnetic tail field hourly average magnitude

distributions in a 10 R_E interval of the tail at the

distance of the moon for Kp ≤ 2 and Kp > 2 during 1967-

1968. Median magnitude is indicated above each

distribution. The only magnitude value exceeding 20γ

for Kp > 2 was in the interval 24-25γ.

Figure 2 Field magnitude distributions at the lunar distance for

Kp ≤ 2 and for measurements both inside a region

-4 ≤ Z_{sm} ≤ 8 R_E and outside that region. The

distribution for the inner region extends to both

higher and lower magnitudes than that for the outer

region.

Figure 3 Average variation of tail field magnitude with distance

from the solar magnetospheric XY plane (upper curve).

The lower curve shows the scatter in the hourly average

magnitude values which were averaged to obtain the upper

curve. The magnitude data show a broad region of

depressed fields centered above Z_{sm} = 0.

Figure 4 Summary of tail field elevation angle in solar magnetospheric

coordinates as a function of distance Z_{sm} from the XY

plane. The numbers of hourly values falling within each

of the indicated intervals of φ_{sm} and Z_{sm} are tabulated.

The region of increased positive field component out
of the XY plane coincides with the depressed magnitude
region shown in Figure 3.

Figure 5 Projections on the solar magnetosphere YZ plane of the
positions of Explorer 35 in the tail when either a single
isolated field reversal was observed or a discrete series
of multiple neutral sheet traversals were detected. A
separation of the data into summer (+) and winter (-)
observations is shown and the associated distributions
of all tail data during those months according to Z_{sm}.
position are shown along the sides.

Figure 6 Variation of the solar-magnetospheric azimuthal angle of
the tail field with distance from the XZ plane, with the
polarity of field lines suppressed. The tilted orientation
of the linear fit to the distribution and the displacement
of the point at which that line has a value of $360^{\circ}/180^{\circ}$
to the negative side of $Y_{sm} = 0$ demonstrate both the
divergence of the tail field with distance from the earth
and the aberration of the field.

Figure 7 Projections on the solar-magnetosphere YZ plane of trajectory
intervals when Explorers 33 and 35 observed the magnetotail
boundary near the orbital distance of the moon. Reference

circle shows aberration of the tail and the mean radius
at which traversals along the dawn and dusk flanks occurred.
Explorer 33 measurements near $Z_{sm} = 30$ R_E suggest an
elliptical cross-section for the tail.

Figure 8 Comparison of observed gradient of the tail field magnitude
with gradients computed using tail field divergence and
average solar magnetospheric B_Z component results. As
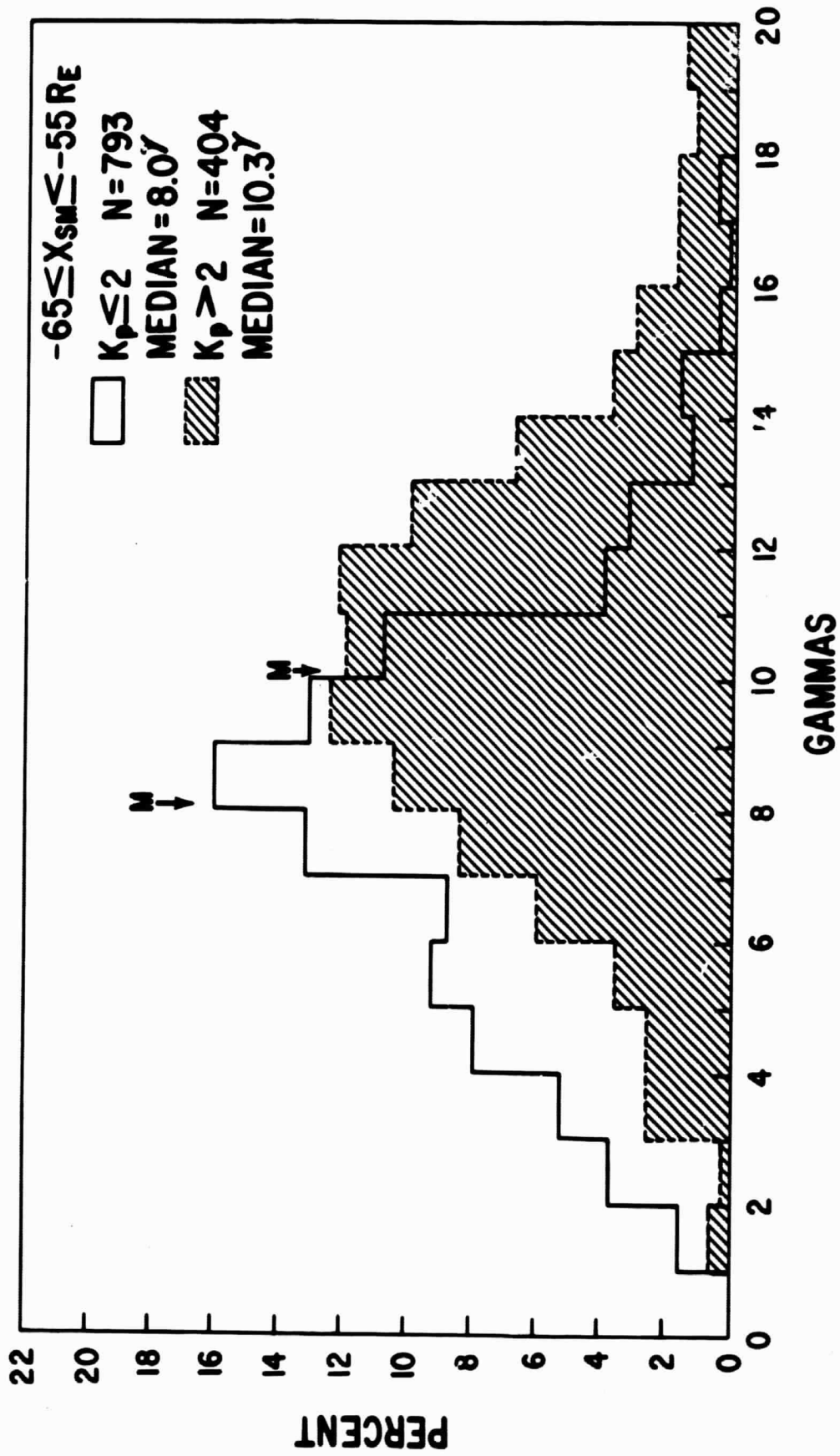can be seen only a combination of the two effects
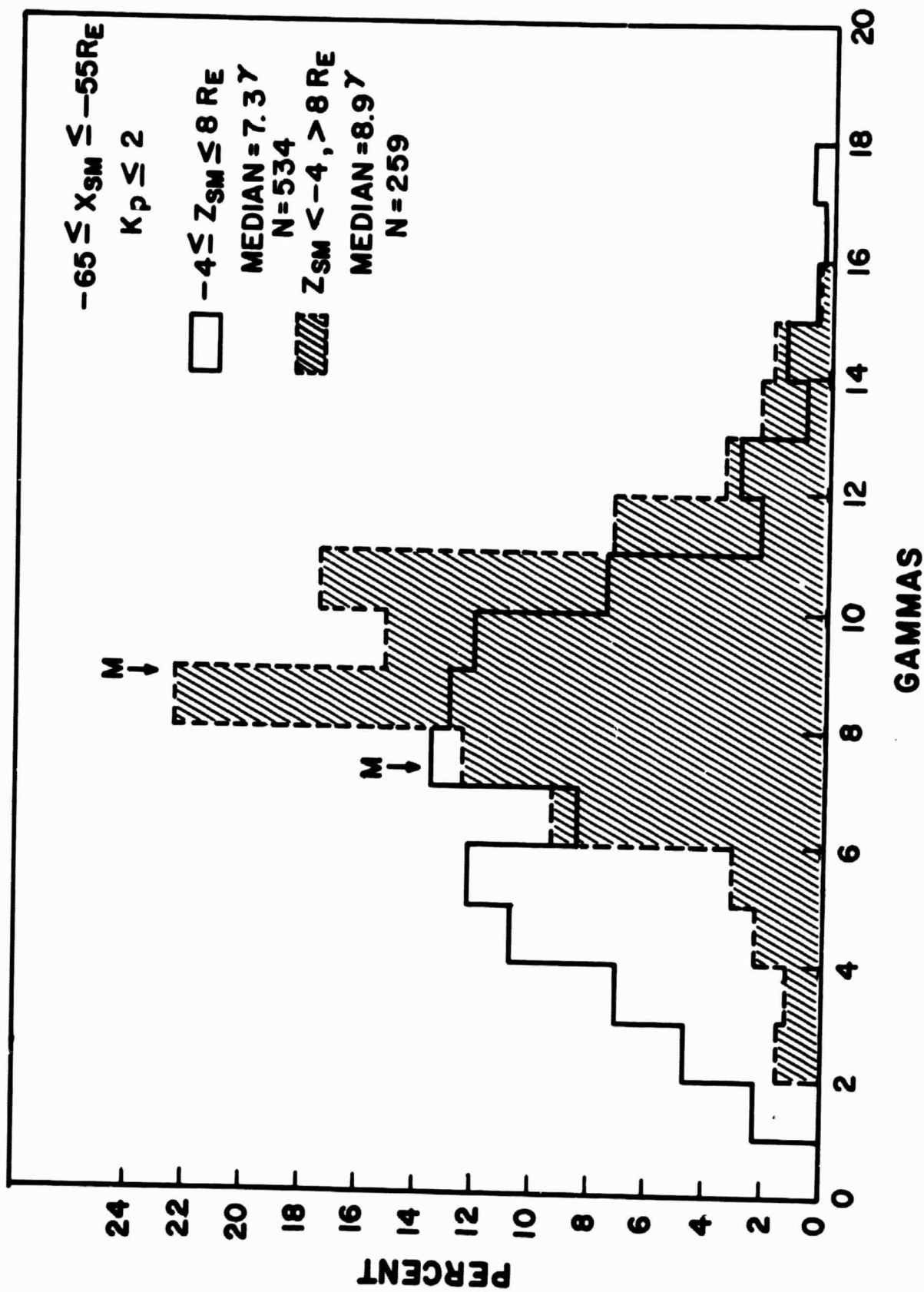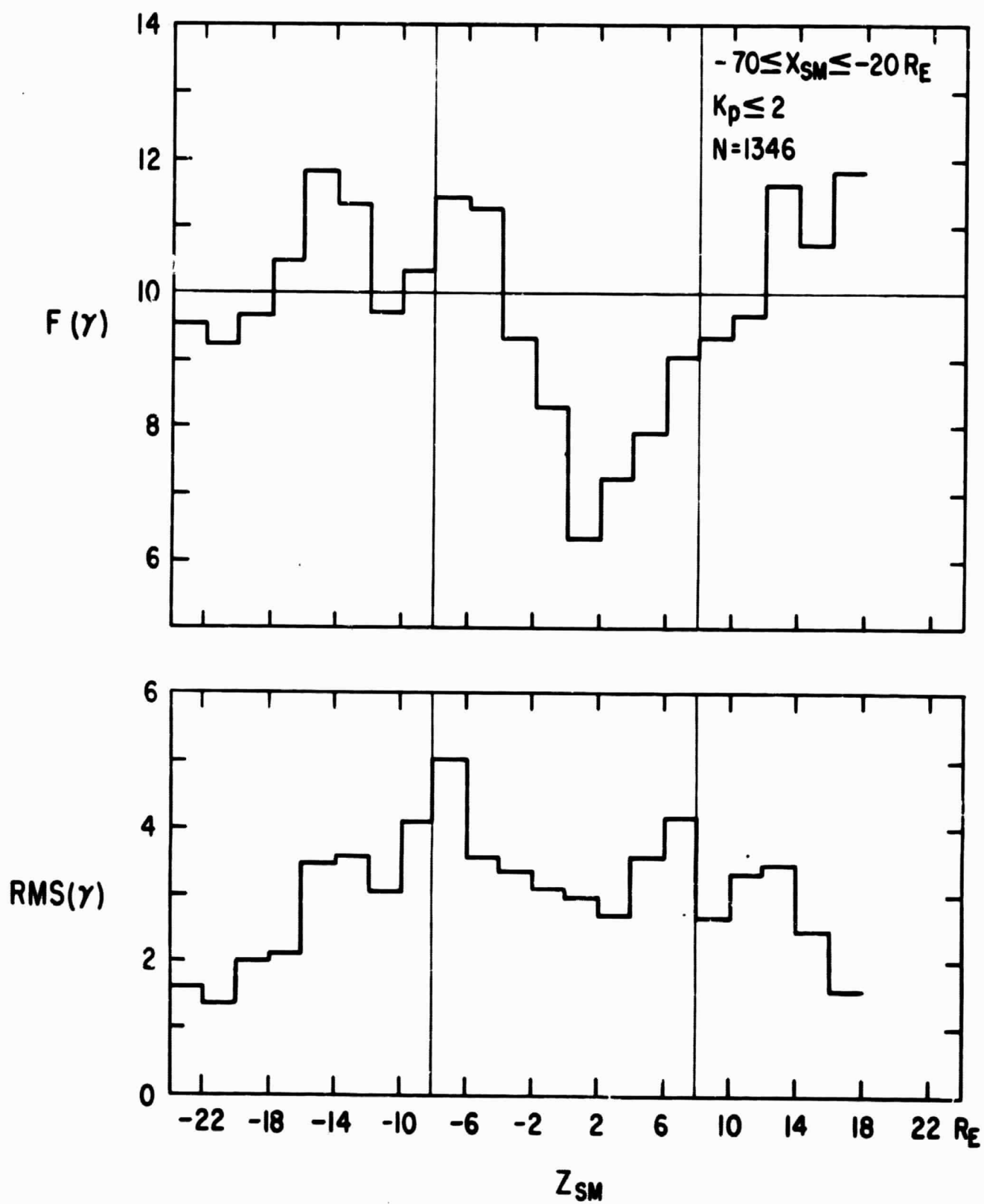adequately describes the measured gradient.
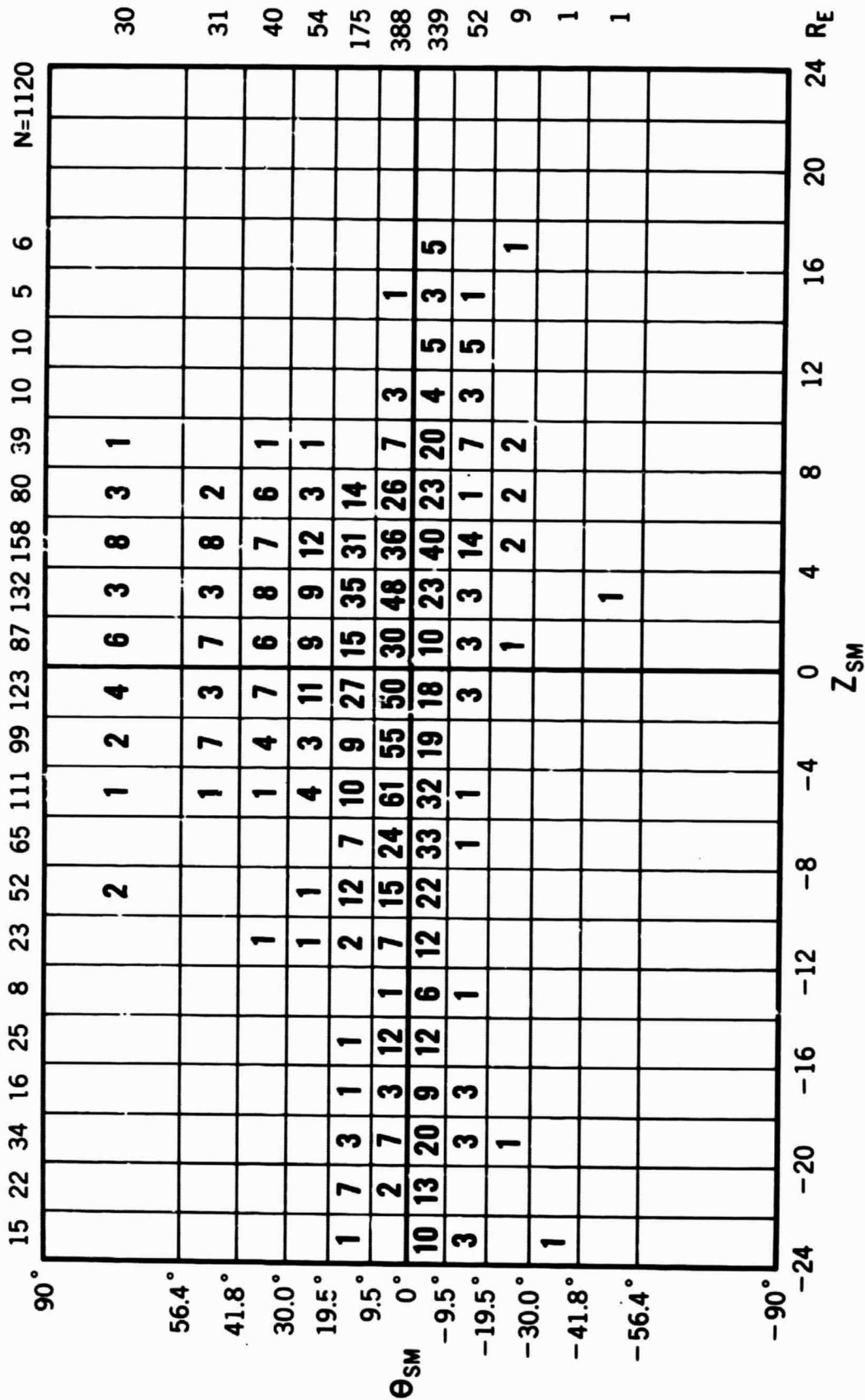
FIGURE 1

FIGURE 2

FIGURE 3

Figure 4 — Distribution of observations in the Z_{SM} – Θ_{SM} plane. Total $N = 1120$.

Column totals (top, left → right, versus Z_{SM}):
15 22 34 16 25 8 23 52 65 111 99 123 87 132 158 80 39 10 10 5 6

Bottom axis Z_{SM} (R$_E$): −24 −20 −16 −12 −8 −4 0 4 8 12 16 20 24

Row totals (right, versus Θ_{SM}):

Θ_{SM}	Row total
90°	
56.4°	30
41.8°	31
30.0°	40
19.5°	54
9.5°	175
0°	388
−9.5°	339
−19.5°	52
−30.0°	9
−41.8°	1
−56.4°	1
−90°	

Observation matrix (rows Θ_{SM}, entries ordered approximately left → right across Z_{SM}):

Θ_{SM}	entries (as printed)
56.4°	2 … 2 4 3 8 3 1
41.8°	1 … 7 3 7 8 2 1
30.0°	1 1 … 4 7 6 8 7 6 1
19.5°	1 … 1 4 3 11 9 12 3 1
9.5°	1 3 1 1 2 12 7 10 27 15 35 31 14
0°	10 13 2 7 15 24 61 55 50 48 36 26 7 3
−9.5°	3 20 9 12 22 33 32 19 18 10 23 40 23 20 4 5 3
−19.5°	3 3 1 1 3 3 14 1 7 3 5 1
−30.0°	2 2 2 1
−41.8°	1
−56.4°	1

FIGURE 4

EXPLORER 35 NEUTRAL SHEET OBSERVATIONS
1967–1968
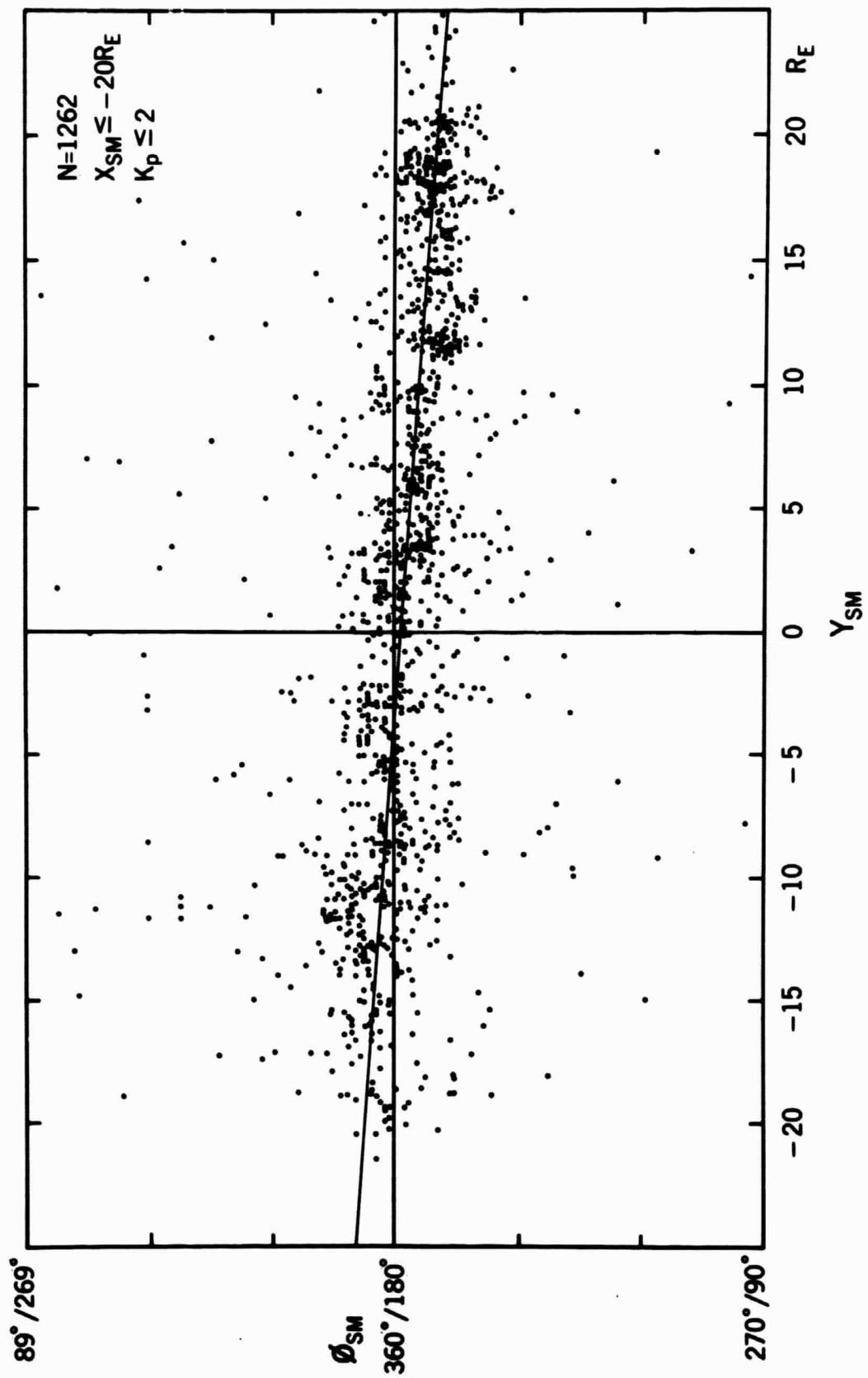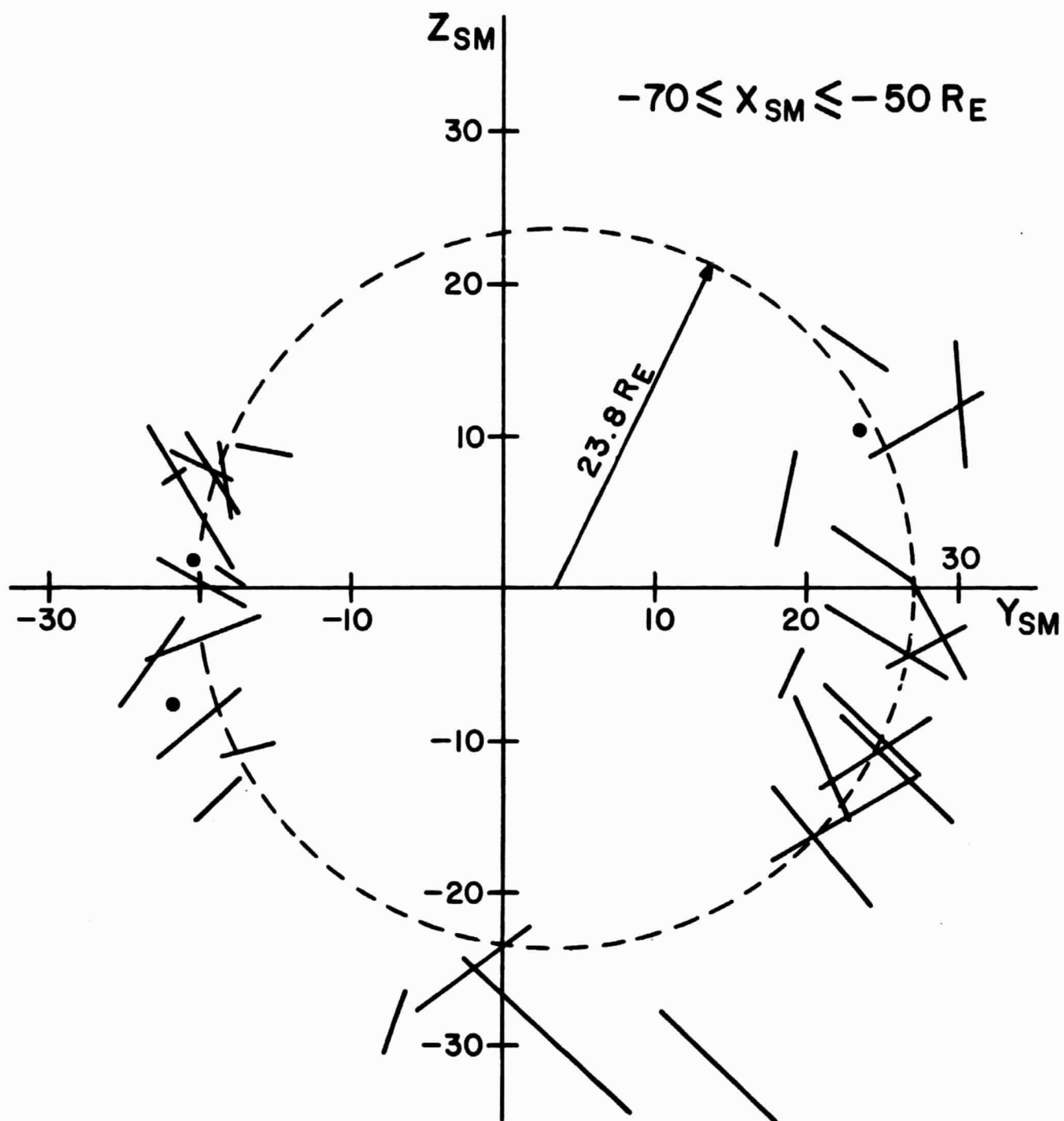
FIGURE 5

+ MAY–JULY   ● NOV.–JAN.

FIGURE 6

MAGNETOTAIL BOUNDARY TRAVERSALS
EXPLORERS 33 & 35, 1967-68

FIGURE 7

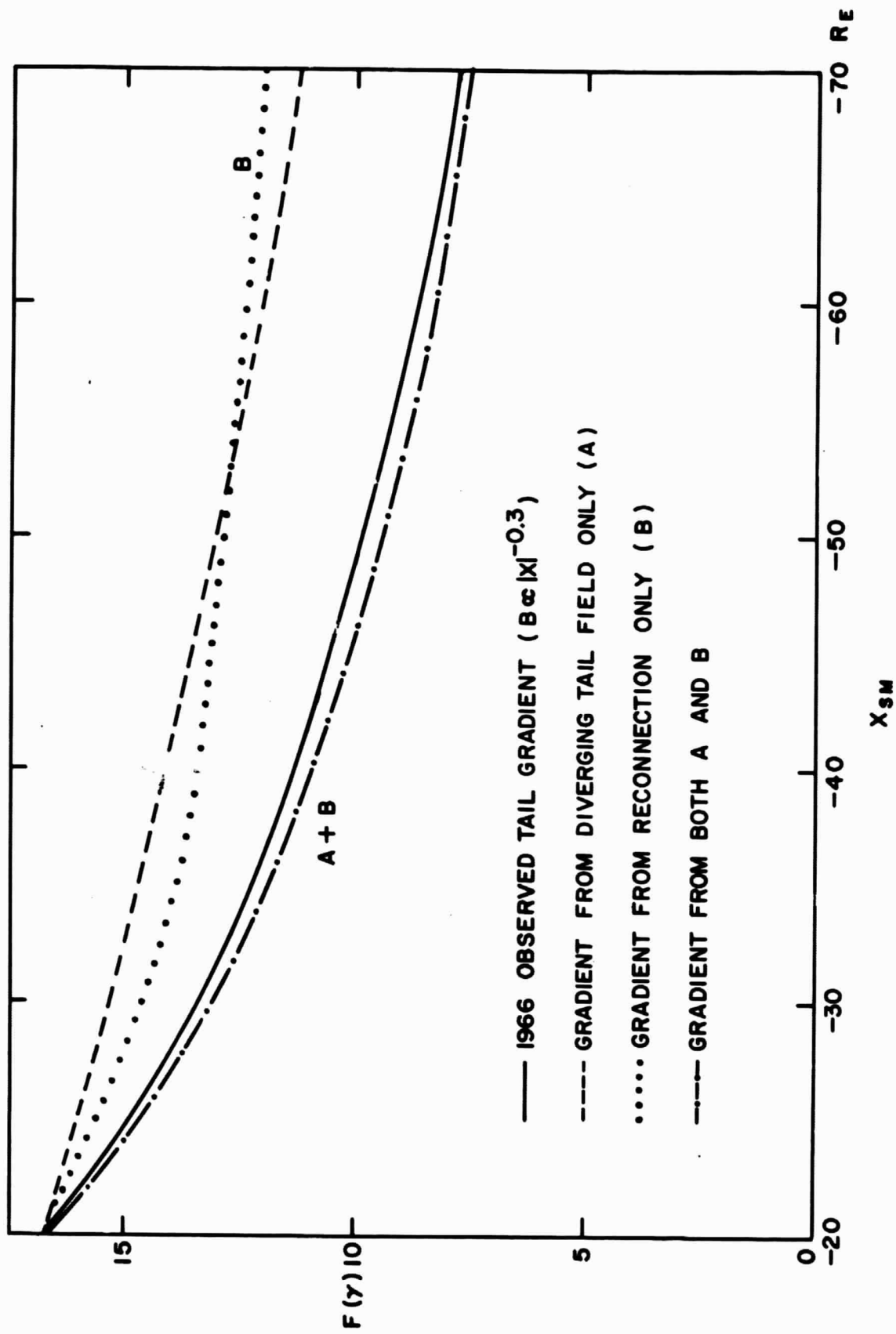FIGURE 8